Accessing the shape of atomic nuclei with relativistic collisions of isobars

Giuliano Giacalone, Jiangyong Jia, and Vittorio Somà

Phys. Rev. C **104**, L041903 — Published 20 October 2021

DOI: 10.1103/PhysRevC.104.L041903

Accessing the shape of atomic nuclei with relativistic collisions of isobars

Giuliano Giacalone,[1] Jiangyong Jia,[2,3] and Vittorio Somà[4]

[1] *Institut für Theoretische Physik, Universität Heidelberg, Philosophenweg 16, 69120 Heidelberg, Germany*
[2] *Department of Chemistry, Stony Brook University, Stony Brook, NY 11794, USA*
[3] *Physics Department, Brookhaven National Laboratory, Upton, NY 11976, USA*
[4] *IRFU, CEA, Université Paris-Saclay, 91191 Gif-sur-Yvette, France*

Nuclides sharing the same mass number (isobars) are observed ubiquitously along the stability line. While having nearly identical radii, stable isobars can differ in shape, and present different quadrupole deformations. We show that even small differences in these deformations can be probed by relativistic nuclear collisions experiments, where they manifest as deviations from unity in the ratios of elliptic flow coefficients taken between isobaric systems. Collider experiments with isobars represent, thus, a unique means to gain precise knowledge of the geometric shape of atomic nuclei.

Introduction. A remarkable connection between low- and high-energy nuclear physics has been recently established in collider experiments conducted at the BNL Relativistic Heavy Ion Collider (RHIC) and at the CERN Large Hadron Collider (LHC) with the realization that the output of relativistic nuclear collisions is strongly affected by the deformation of the colliding ions.

The key observable driving this finding is elliptic flow, the quadrupole deformation (second Fourier harmonic) of the azimuthal distribution of hadrons detected in the final state of relativistic nuclear collisions [1]:

$$V_2 \propto \int_{\rm detector} f(\varphi) e^{i2\varphi}, \tag{1}$$

where $f(\varphi)$ is the distribution of azimuthal angles (in momentum space) collected in a collision event.

In nucleus-nucleus collisions, elliptic flow emerges as a response to the quadrupole asymmetry (ellipticity) of the system created, right after the interaction takes place, in the plane transverse to the beam direction [2]:

$$\mathcal{E}_2 \propto \int_{\rm overlap\ area} \epsilon(r,\phi)\ r^2 e^{i2\phi}, \tag{2}$$

where (r,ϕ) parametrize the transverse plane (for simplicity at $z=0$), and ϵ is the density of energy deposited in the overlap. In full generality, $\mathcal{E}_2 \neq 0 \Rightarrow V_2 \neq 0$. As illustrated in the left panel of Fig. 1, any collision occurring at finite impact parameter presents an overlap area which carries an elliptical deformation, i.e., $\mathcal{E}_2 \neq 0$, explaining in particular the observation that V_2 grows steeply with the collision impact parameter.

However, for the majority of isotopes, even in the limit of vanishing impact parameter one expects $\mathcal{E}_2 \neq 0$, and thus $V_2 \neq 0$ from nuclear structure arguments. Most of nuclei present in fact a nonvanishing intrinsic quadrupole moment, i.e., an ellipsoidal deformation [3]:

$$Q_{20} \propto \int_{\rm nucleus} \rho(r,\Theta,\Phi)\ r^2 Y_{20}(\Theta,\Phi), \tag{3}$$

where $\rho(r,\Theta,\Phi)$ represents the nucleon density in the intrinsic frame of the nucleus. Ultrarelativistic collisions take snapshots of randomly-oriented configurations of nucleons at the time of interaction, so that, if the colliding ions present $Q_{20} \neq 0$, regions of overlap such as that proposed in the right panel of Fig. 1 can be produced. These lead to $\mathcal{E}_2 \neq 0$ at zero impact parameter.

The bottom line is that in nucleus-nucleus collisions:

$$Q_{20} \neq 0 \quad \Longrightarrow \quad \mathcal{E}_2 \neq 0 \quad \Longrightarrow \quad V_2 \neq 0. \tag{4}$$

The importance of this statement has been recently clarified in the context of ^{238}U+^{238}U collisions at RHIC, with the realization that observables based on V_2 (and on the hadron mean transverse momentum, $\langle p_t \rangle$) are essentially dominated by effects due to the deformed shape of uranium nuclei [4, 5], and at LHC with the measurement of an abnormally large V_2 in ^{129}Xe+^{129}Xe collisions compared to ^{208}Pb+^{208}Pb collisions [6–8].

These discoveries naturally trigger the question of whether one can use the great resolving power of high-energy colliders to infer something new about the low-energy structure of nuclei, and provide a new means to test state-of-the-art approaches to the nuclear many-body problem. In this Letter, we show that this is possible, and how such a goal can be pursued experimentally.

The idea. We exploit the seemingly uninteresting fact that a large number of stable nuclides belong to pairs of isobars, i.e., that for a given nuclide X one can often find a different nuclide Y that contains the same number of nucleons. This feature has an important implication for high-energy collisions. If X and Y are isobars, then X+X collisions produce a system which has the same properties (volume, density) as that produced in Y+Y collisions. As a consequence, X+X and Y+Y systems present the same geometry, the same dynamical evolution, and thus the same elliptic flow in the final state.

Given isobars X and Y, we ask, hence, the following:

$$\boxed{\frac{v_2\{2\}_{\rm X+X}}{v_2\{2\}_{\rm Y+Y}} \stackrel{?}{=} 1} \tag{5}$$

where $v_2\{2\}$ represents the usual rms measure of the magnitude of V_2 in a given multiplicity class. As argued above, the ratio should be equal to 1. Experimentally, once a number of minimum bias collisions of order 10^8 is available, the ratio at small centralities can be obtained free of statistical error, while systematic uncertainties cancel in the ratio if the detector conditions of the X+X and Y+Y runs are the same [9]. Corrections to the ratio in Eq. (5) can further appear if the systems produced in X+X and Y+Y collisions have different sizes, for instance, due to the fact that X and Y present different neutron numbers. However, two stable isobars can differ in matter radius by at most 0.5% [10], leading to a small correction. For the isobars collided at RHIC in 2018, ^{96}Ru and ^{96}Zr, deviations from unity in the ratio of v_2 coefficients have been analyzed in Ref. [11], for different models of the nucleon density. In central collisions and for spherical nuclei, it was found that the deviation from unity is at maximum 1%. A deviation as large as 2% appears, on the other hand, in peripheral collisions, due to the different diffusivity [see a in Eq. (6)] of the two isobars [12, 13]. This effect is however pronounced (>1%) only at large impact parameters, where nuclear deformation does not influence the rms elliptic flow.

For central collisions, significant deviations (>1%) from unity in the ratio of the v_2 coefficients can only arise from the different deformations of the isobars. Deformation reflects the collective organization of nucleons in the nuclear ground state, and it varies with proton and neutron numbers. In general, one does not expect two stable isobars to present the same deformation. The point we want to make in this Letter is, then, the following:

> *Given two isobars, X and Y, if one measures* $\frac{v_2\{2\}_{\rm X+X}}{v_2\{2\}_{\rm Y+Y}} > 1$ *in central collisions, with a deviation from unity larger than 1%, then one must conclude that X has a larger intrinsic quadrupole deformation than Y.*

This statement is based on two facts: (*i*) that elliptic flow emerges from the elliptic anisotropy of the overlap area; (*ii*) that nuclei in their ground states typically have nonvanishing intrinsic quadrupole moments. These are established features of nuclear physics that do not rely on any specific approximation or model.

Therefore, through measurements of the ratio in Eq. (5) one obtains a qualitative information about the relative deformation of the isobars which, as we show in the following, can be turned into a quantitative one, as even small differences in the quadrupole deformation of two isobars give rise to unambiguous and detectable effects in the ratio of the v_2 coefficients. As mentioned above, this ratio is virtually devoid of experimental error and systematically accessible, under the same experimental conditions, throughout the Segrè chart. Such features are hardly attainable in low-energy nuclear structure experiments. Therefore, collider data will challenge the predictions of nuclear models tuned to low-energy experimental data in an unprecedented way.

Application. To get some intuition about the kind of results that will be obtained in collider experiments, we now perform quantitative calculations of Eq. (5) by means of models, namely, a standard parametrization for the deformed nuclear matter density, and a Glauber-type model for the collision process.

A common parametrization of the nucleon density is the 2-parameter Fermi (2pF) distribution:

$$\rho(r,\Theta,\Phi) \propto \frac{1}{1+\exp\left(\left[r-R(\Theta,\Phi)\right]/a\right)}, \tag{6}$$

where a denotes the surface diffuseness and the half-density radius R carries information about the deformed shape. We characterize R through a spherical harmonic expansion: $R(\Theta,\Phi) = R_0\left[1+\beta Y_{2,0}(\Theta,\Phi)\right]$, truncated at the axial quadrupole, $Y_{2,0}$, as corrections to $v_2\{2\}$ due to triaxial, $Y_{2,\pm 2}$, and hexadecapole, $Y_{4,0}$, deformations are negligible in the limit of central collisions [14]. The coefficient β quantifies[1] the ellipsoidal shape of the nucleus:

$$\beta \simeq \frac{4\pi}{5} \frac{\int \rho(r,\Theta,\Phi)\ r^2 Y_{20}(\Theta,\Phi)}{\int \rho(r,\Theta,\Phi)\ r^2}. \tag{7}$$

Well-deformed nuclei, such as ^{238}U, or the stable nuclides with $150 < A < 180$, are characterized by $\beta \approx 0.3$.

Two nuclei, described as randomly oriented, deformed batches of nucleons sampled independently according to the 2pF distribution given in Eq. (6), are then collided at ultrarelativistic energy. On a collision-by-collision basis, the energy density deposited in the process possesses a nonvanishing eccentricity, $\varepsilon_2 \equiv |\mathcal{E}_2|$, which triggers the development of elliptic flow during the expansion of the system, resulting in the observed momentum anisotropy, V_2. Dubbing $v_2 \equiv |V_2|$, at a given multiplicity (centrality) one has: $v_2 = \kappa_2 \varepsilon_2$, where κ_2 is a real coefficient that depends on the properties of the system (e.g., equation of state and viscosity in a hydrodynamic model [1]). As anticipated, isobaric systems share the same physical properties, so that a crucial simplification occurs: $\kappa_2[\mathrm{X}+\mathrm{X}] = \kappa_2[\mathrm{Y}+\mathrm{Y}]$. In the ratio between v_2 coefficients calculated in two different isobaric systems, then, the response κ_2 drops out. This in turn implies that:

$$\frac{v_2\{2\}_{\mathrm{X+X}}}{v_2\{2\}_{\mathrm{Y+Y}}} = \frac{\varepsilon_2\{2\}_{\mathrm{X+X}}}{\varepsilon_2\{2\}_{\mathrm{Y+Y}}} \stackrel{?}{=} 1. \tag{8}$$

The question of whether or not the measured ratio of v_2 coefficients is equal to unity boils down to whether the two isobaric system possess the same fluctuations of ε_2.

This allows us now to employ a collision model to calculate Eq. (8), and thus to perform a quantitative evaluation of the ratio of the v_2 coefficients to be measured at colliders. To do so, we use the default TRENTo model [17], which has proven able to capture with good accuracy the effects of the quadrupole deformation of nuclei on elliptic flow data collected in ^{238}U+^{238}U collisions. We perform this analysis for two pairs of isobars:

- A pair of well-deformed nuclei, namely, ^{154}Sm and ^{154}Gd. For the 2pF density profile, we assume that the matter distribution is identical to the measured charge density, a good approximation for stable nuclides. For both nuclei we employ $R = 5.975$ fm and $a = 0.59$ fm Ref. [18]. For the deformation parameters, we adopt values inferred from the measured transition probabilities of the electric quadrupole operator from the ground state to the first 2^+ state, tabulated, e.g., in Ref. [19]. One finds[2] $\beta = 0.34$ for ^{154}Sm and $\beta = 0.31$ for ^{154}Gd.

- A pair of lighter nuclei, ^{96}Zr and ^{96}Ru, of great relevance since ^{96}Zr+^{96}Zr and ^{96}Ru+^{96}Ru collisions have been performed at RHIC in 2018 [9], and experimental results will be released shortly. For the 2pF of these nuclei we set $R = 5.06$ fm for ^{96}Zr and $R = 5.03$ fm for ^{96}Ru, taking into account the fact that ^{96}Zr has an excess of 4 neutrons, while $a = 0.52$ fm for both. The deformation parameters are $\beta = 0.15$ for ^{96}Ru, and $\beta = 0.06$ for ^{96}Zr [19].

For each system we simulate 5 million minimum bias collisions. We sort events into centrality classes according to the entropy created in the process, following the default TRENTo prescription. In each centrality bin, we evaluate $\varepsilon_2\{2\}$, and by subsequently taking the ratio of Eq. (8), we obtain the results displayed in Fig. 2.

The shaded band corresponds to a departure from unity smaller than 1%. We interpret any deviation falling outside the band as a genuine signature of the different quadrupole deformations carried by the two isobars, although we caution that for precise comparisons with future data, uncertainties related to the centrality definition of our model will have to be carefully addressed [21, 22]. The black solid line represents our result for the systems collided in 2018 at RHIC. It is consistent with a similar calculation done in Ref. [23], and can be confronted with upcoming data. For our choice of the deformation parameters, we observe that the splitting between the flow coefficients in central collisions is well above 1%, consistent with the fact that ^{96}Ru has a larger quadrupole deformation. The same behavior is observed for the pair of heavier nuclei (red dashed line), where a deviation from unity of order 5% emerges in central collisions, reflecting the larger deformation of ^{154}Sm nuclei.

The fact that both pairs return a similar (small) splitting between v_2 coefficients can be understood as follows. At a given centrality, one expects [24, 25]:

$$\varepsilon_2\{2\}^2 = a_0 + a_1 \beta^2. \tag{9}$$

[1] We assume here that nuclei have a fixed quadrupole deformation, though shape fluctuations are normally present, depending on the "softness" of the nuclear system (see e.g. Ref. [15]). We have checked that the quantitative results presented in this section do not change significantly if a distribution in β is considered instead of the fixed value stated below [16].

[2] These results rely on approximations (e.g., a sharp nuclear surface) that are not fully consistent with the use of Eq. (6). We neglect this possible mismatch, typically of order 5-10% [20].

The coefficient a_0 is the eccentricity due to nucleon positions, while the term proportional to β^2 represents the contribution from fluctuations in the orientation of the deformed ions. Systems X+X and Y+Y have the same size and number of participant nucleons, therefore, they present the same a_0 and a_1. In the T$_\mathrm{R}$ENTo results we find that, even for $A = 154$ and $\beta \approx 0.3$, the contribution from a_0 to Eq (9) is larger than the contribution from $a_1\beta^2$. Inserting Eq. (9) in Eq. (8), expanding the ratio around unity, and keeping the leading correction, equation (8) becomes:

$$\frac{v_2\{2\}_{\mathrm{X+X}}}{v_2\{2\}_{\mathrm{Y+Y}}} \simeq 1 + \frac{c}{2}\left(\beta_{\mathrm{X}}^2 - \beta_{\mathrm{Y}}^2\right), \tag{10}$$

where c gives the relative variation of the ms eccentricity with β^2, $c = d\left(\ln \varepsilon_2\{2\}^2\right)/d\beta^2|_{\beta_{\mathrm{Y}}^2}$. For both pairs in our application one has $\beta_X^2 - \beta_Y^2 \approx 0.02$, and $c \approx 6$, explaining the similarity between the curves in Fig. 2.

We note that c is a property of the geometry of the system, whose uncertainty can be quantified from initial condition models. This means that in high-energy experiments one can extract the difference $\beta_{\mathrm{X}}^2 - \beta_{\mathrm{Y}}^2$ with a well-defined theoretical error. As the way $\varepsilon_2\{2\}^2$ depends on β is largely model-independent [25], this error will be small. Therefore, while heavy-ion collisions may not yet provide a simple way to extract the value of β from collisions of a given species, the extraction of relative information, involving more than one system, is remarkably robust, and leads to a knowledge of precision comparable to that obtained from low-energy measurements. Such knowledge is fully complementary to the existing one, albeit free from uncertainties appearing in the translation of spectroscopic information into shape parameters. High-energy collisions can be performed, for instance, with any nucleus, even or odd, while it is not possible to unambiguously assign a meaning in terms of geometric shapes to spectroscopic data for isotopes containing either an odd number of protons or neutrons.

Our most important result concerns the heavier species with $A = 154$. The contribution from the nuclear deformation in Eq. (9) is quadratic in β, therefore, it is much more important for well-deformed nuclei, $\beta \approx 0.3$. For this reason, as found in Fig. 2, for well-deformed nuclei even percent-level differences in the values of β will leave visible signatures in the ratio of flow coefficients. In this scenario, the qualitative statement that X is more deformed than Y turns into a nontrivial quantitative issue, driven by tiny differences in the shape of the isobars.

Conclusion & Outlook. Relativistic collision experiments involving stable isobars, such as ^{96}Zr+^{96}Zr and ^{96}Ru+^{96}Ru collisions recently run at RHIC, yield ratios of v_2 coefficients between isobaric systems that are not simply equal to one, but rather look like the curves shown in Fig. 2. A given ratio falling outside the shaded band indicates that the geometric shapes of the colliding ions are different. This information is virtually free of experimental error. It has to be confronted with our knowledge of nuclear physics across energy scales and can be accessed systematically across the nuclide chart thanks to the abundance of stable isobars found in Nature.

Physicists should take advantage of this opportunity. All pairs and triplets of isobars which are stable enough to be used in potential collider experiments are listed in Tab. I. Well-deformed nuclei are highlighted in a red box. A recent study [26] further suggests that ^{146,148,150}Nd and ^{150}Sm may present an octupole deformation ($Q_{30} \propto \int r^3 Y_{30}(\Theta,\Phi)\rho(r,\Theta,\Phi) \neq 0$) in their ground state. A small octupole deformation would be visible in high-energy collisions as an enhancement of the fluctuations of triangular flow, v_3 [14, 27]. Therefore, Nd and Sm isotopes represent ideal candidates for such a study.

These experiments can be repeated for several pairs of isotopes in identical conditions, and provide us with an information independent of specific nuclear structure details. High-energy collisions represent, thus, a tool truly complementary to modern low-energy experiments. They offer a unique way to test the predictions of nuclear models for a wide range of species, and consequently pose a solid baseline for the next generation of theory-to-data comparisons involving *ab-initio* frameworks of nuclear structure currently under intense development [28].

Note added. During the process of publication of this manuscript, the STAR collaboration has released experimental data on ratios of flow coefficients in ^{96}Zr+^{96}Zr and ^{96}Ru+^{96}Ru collisions [29]. The enhancement of v_2 in ^{96}Ru+^{96}Ru collisions predicted in Fig. 2 has been observed. Additionally, a strong enhancement of v_3 in ^{96}Zr+^{96}Zr collisions has been reported. This suggests the presence of an octupole deformation in the ground state of ^{96}Zr. This conclusion seems consistent with low-energy spectroscopic measurements that have identified a low-lying 3^- state with a large B(E3) transition strength in such nuclei [30], pointing to octupole collectivity. Yet, the theoretical description of such correlations in the ground state of ^{96}Zr represents a challenge for state-of-the-art theoretical frameworks (see, e.g., [26, 31] and the discussion in [30]). These findings corroborate our point that colliding isobars at high energy provides a new type of information on the shape of nuclei and can critically reinforce or challenge analyses of low-energy data.

Acknowledgments. We thank the participants of the Initial Stages 2021 conference, in particular Jaki Noronha-Hostler, Sören Schlichting, and Peter Steinberg for inspiring comments on the subject of this work. G.G. acknowledges discussions with Benjamin Bally, Michael Bender, and Matt Luzum. V.S. additionally thanks Magdalena Zielińska for useful discussions. G.G. is supported by the Deutsche Forschungsgemeinschaft (DFG, German Research Foundation) under Germanys Excellence Strategy EXC 2181/1 - 390900948 (the Heidelberg STRUCTURES Excellence Cluster), SFB 1225 (ISOQUANT) and FL 736/3-1. The work of J.J is supported by DOE DEFG0287ER40331 and NSF PHY-1913138.

---

[1] U. Heinz and R. Snellings, Ann. Rev. Nucl. Part. Sci. **63**, 123 (2013) doi:10.1146/annurev-nucl-102212-170540 [arXiv:1301.2826 [nucl-th]].
[2] D. Teaney and L. Yan, Phys. Rev. C **83**, 064904 (2011) doi:10.1103/PhysRevC.83.064904 [arXiv:1010.1876 [nucl-th]].
[3] A. Bohr and B. Mottelson, *Nuclear Structure*, Vol. I (W. A. Benjamin Inc., 1969; World Scientific, 1998).
[4] L. Adamczyk *et al.* [STAR Collaboration], Phys. Rev. Lett. **115**, no. 22, 222301 (2015) doi:10.1103/PhysRevLett.115.222301 [arXiv:1505.07812 [nucl-ex]].
[5] J. Jia, contribution to the VI$^{\text{th}}$ International Conference on the Initial Stages of High-Energy Nuclear Collisions (IS21), `https://indico.cern.ch/event/854124/contributions/4135480/`
[6] S. Acharya *et al.* [ALICE Collaboration], Phys. Lett. B **784**, 82 (2018) doi:10.1016/j.physletb.2018.06.059 [arXiv:1805.01832 [nucl-ex]].
[7] A. M. Sirunyan *et al.* [CMS Collaboration], Phys. Rev. C **100**, no. 4, 044902 (2019) doi:10.1103/PhysRevC.100.044902 [arXiv:1901.07997 [hep-ex]].
[8] G. Aad *et al.* [ATLAS Collaboration], Phys. Rev. C **101**, no. 2, 024906 (2020) doi:10.1103/PhysRevC.101.024906 [arXiv:1911.04812 [nucl-ex]].
[9] J. Adam *et al.* [STAR Collaboration], Nucl. Sci. Tech. **32**, no. 5, 48 (2021) doi:10.1007/s41365-021-00878-y [arXiv:1911.00596 [nucl-ex]].
[10] H. Li, H. j. Xu, Y. Zhou, X. Wang, J. Zhao, L. W. Chen and F. Wang, Phys. Rev. Lett. **125**, no. 22, 222301 (2020) doi:10.1103/PhysRevLett.125.222301 [arXiv:1910.06170 [nucl-th]].
[11] H. Li, H. j. Xu, J. Zhao, Z. W. Lin, H. Zhang, X. Wang, C. Shen and F. Wang, Phys. Rev. C **98**, no. 5, 054907 (2018) doi:10.1103/PhysRevC.98.054907 [arXiv:1808.06711 [nucl-th]].
[12] H. J. Xu, X. Wang, H. Li, J. Zhao, Z. W. Lin, C. Shen and F. Wang, Phys. Rev. Lett. **121**, no. 2, 022301 (2018) doi:10.1103/PhysRevLett.121.022301 [arXiv:1710.03086 [nucl-th]].
[13] H. j. Xu, H. Li, X. Wang, C. Shen and F. Wang, arXiv:2103.05595 [nucl-th].
[14] J. Jia, [arXiv:2106.08768 [nucl-th]].
[15] A. Poves, F. Nowacki and Y. Alhassid, Phys. Rev. C **101**, no.5, 054307 (2020) doi:10.1103/PhysRevC.101.054307 [arXiv:1906.07542 [nucl-th]].
[16] B. Bally, M. Bender, G. Giacalone, V. Somà, in preparation (2021).
[17] J. S. Moreland, J. E. Bernhard and S. A. Bass, Phys. Rev. C **92**, no. 1, 011901 (2015) doi:10.1103/PhysRevC.92.011901 [arXiv:1412.4708 [nucl-th]].
[18] H. De Vries, C. W. De Jager and C. De Vries, Atom. Data Nucl. Data Tabl. **36**, 495 (1987). doi:10.1016/0092-640X(87)90013-1
[19] NuDat database, National Nuclear Data Center (NNDC), `https://www.nndc.bnl.gov/nudat2`
[20] Q. Y. Shou, Y. G. Ma, P. Sorensen, A. H. Tang, F. Videbk and H. Wang, Phys. Lett. B **749**, 215 (2015) doi:10.1016/j.physletb.2015.07.078 [arXiv:1409.8375 [nucl-th]].
[21] J. Jia, C. Zhang and J. Xu, Phys. Rev. Res. **2**, no. 2, 023319 (2020) doi:10.1103/PhysRevResearch.2.023319 [arXiv:2001.08602 [nucl-th]].
[22] M. Aaboud *et al.* [ATLAS Collaboration], JHEP **2001**, 051 (2020) doi:10.1007/JHEP01(2020)051 [arXiv:1904.04808 [nucl-ex]].
[23] W. T. Deng, X. G. Huang, G. L. Ma and G. Wang, Phys. Rev. C **94**, 041901 (2016) doi:10.1103/PhysRevC.94.041901 [arXiv:1607.04697 [nucl-th]].
[24] G. Giacalone, Phys. Rev. C **99**, no. 2, 024910 (2019) doi:10.1103/PhysRevC.99.024910 [arXiv:1811.03959 [nucl-th]].
[25] G. Giacalone, J. Jia and C. Zhang, [arXiv:2105.01638 [nucl-th]].
[26] Y. Cao, S. E. Agbemava, A. V. Afanasjev, W. Nazarewicz and E. Olsen, Phys. Rev. C **102**, no. 2, 024311 (2020) doi:10.1103/PhysRevC.102.024311 [arXiv:2004.01319 [nucl-th]].
[27] P. Carzon, S. Rao, M. Luzum, M. Sievert and J. Noronha-Hostler, Phys. Rev. C **102**, no. 5, 054905 (2020) doi:10.1103/PhysRevC.102.054905 [arXiv:2007.00780 [nucl-th]].
[28] H. Hergert, Front. in Phys. **8**, 379 (2020) doi:10.3389/fphy.2020.00379 [arXiv:2008.05061 [nucl-th]].
[29] M. Abdallah *et al.* [STAR], [arXiv:2109.00131 [nucl-ex]].
[30] Ł. W. Iskra, R. Broda, R. V. F. Janssens, M. P. Carpenter, B. Fornal, T. Lauritsen, T. Otsuka, T. Togashi, Y. Tsunoda and W. B. Walters, *et al.* Phys. Lett. B **788**, 396-400 (2019) doi:10.1016/j.physletb.2018.10.069
[31] L. M. Robledo and G. F. Bertsch, Phys. Rev. C **84**, 054302 (2011) doi:10.1103/PhysRevC.84.054302 [arXiv:1107.3581 [nucl-th]].

FIGURES

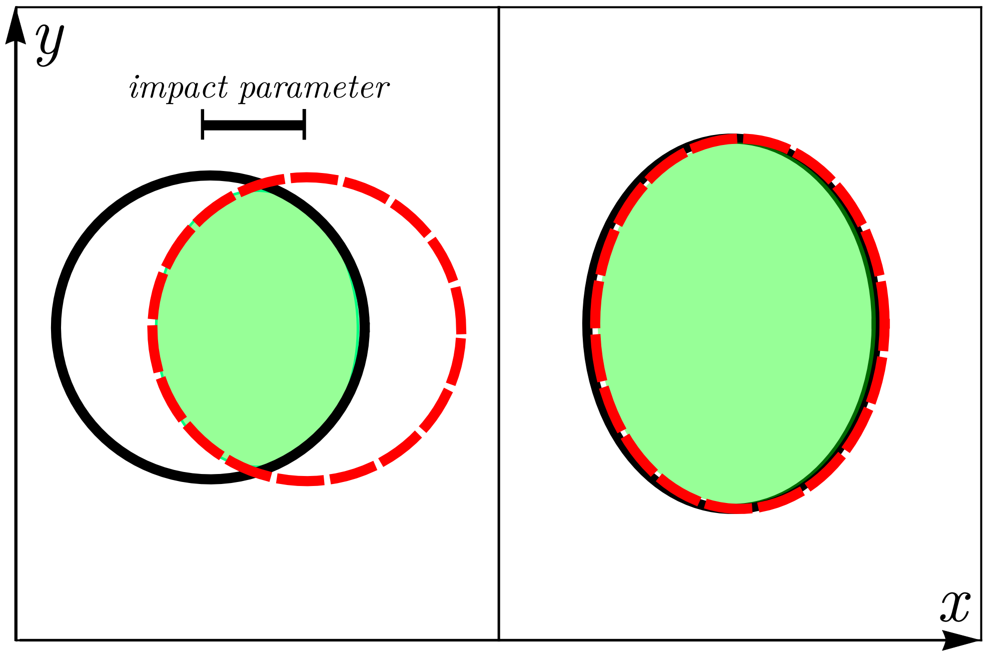

FIG. 1. Anisotropic overlap regions in nuclear collisions. Left: a collision of spherical nuclei breaks anisotropy in the transverse plane due to the finite impact parameter. Right: a central collision of deformed nuclei breaks anisotropy due to the non-spherical shape of the colliding bodies.

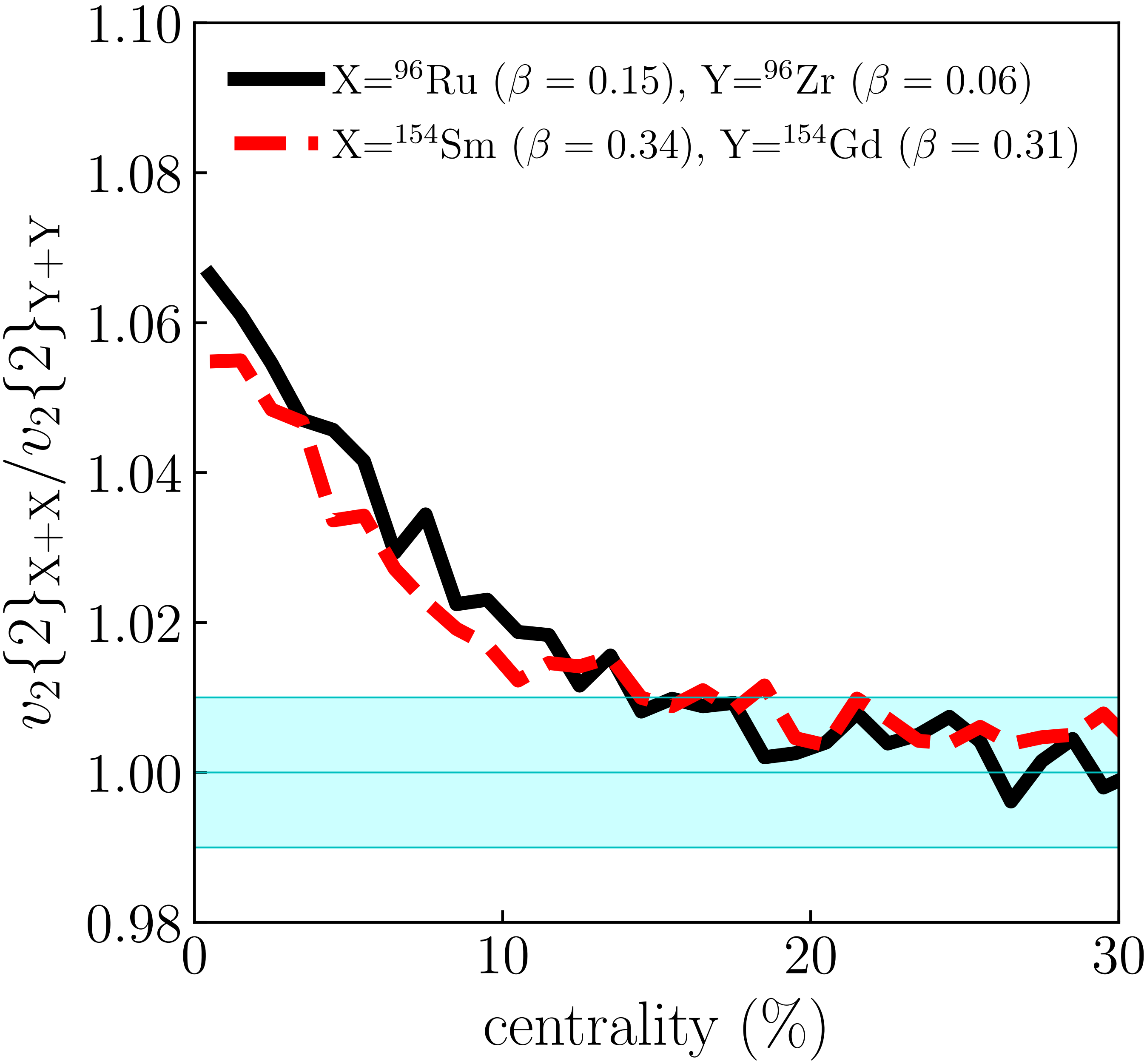

FIG. 2. Rms elliptic flow in X+X collisions divided by the rms elliptic flow in Y+Y collisions as a function of collision centrality. The ratio of flow coefficients is estimated following Eq. (8) and the T$_{\mathrm{R}}$ENTo model. The shaded band represents a 1% deviation from unity. Any deviation from unity which falls outside the shaded band can be considered as a significant signature that $\beta_{\mathrm{X}} \neq \beta_{\mathrm{Y}}$.

TABLES

A	isobars
36	Ar, S
40	Ca, Ar
46	Ca, Ti
48	Ca, Ti
50	Ti, V, Cr
54	Cr, Fe
64	Ni, Zn
70	Zn, Ge
74	Ge, Se
76	Ge, Se
78	Se, Kr
80	Se, Kr
84	Kr, Sr, Mo
86	Kr, Sr
87	Rb, Sr
92	Zr, Nb, Mo
94	Zr, Mo
96	Zr, Mo, Ru
98	Mo, Ru
100	Mo, Ru
102	Ru, Pd
104	Ru, Pd
106	Pd, Cd
108	Pd, Cd
110	Pd, Cd
112	Cd, Sn
113	Cd, In
114	Cd, Sn
115	In, Sn
116	Cd, Sn
120	Sn, Te
122	Sn, Te
123	Sb, Te
124	Sn, Te, Xe
126	Te, Xe
128	Te, Xe
130	Te, Xe, Ba
132	Xe, Ba
134	Xe, Ba
136	Xe, Ba, Ce
138	Ba, La, Ce
142	Ce, Nd
144	Nd, Sm
146	Nd, Sm
148	Nd, Sm
150	Nd, Sm
152	Sm, Gd
154	Sm, Gd
156	Gd, Dy
158	Gd, Dy

160	Gd, Dy
162	Dy, Er
164	Dy, Er
168	Er, Yb
170	Er, Yb
174	Yb, Hf
176	Yb, Lu, Hf
180	Hf, W
184	W, Os
186	W, Os
187	Re, Os
190	Os, Pt
192	Os, Pt
198	Pt, Hg
204	Hg, Pb

TABLE I. Pairs and triplets of stable isobars (half-life longer than 10^8 y). A total of 139 nuclides are listed. The region marked in red contains large well-deformed nuclei ($\beta > 0.2$). The region marked in blue corresponds to nuclides which may present an octupole deformation in their ground state [26].